ISSN 1063-7842, Technical Physics, 2016, Vol. 61, No. 9, pp. 1418–1422. © Pleiades Publishing, Ltd., 2016.
Original Russian Text © A.S. Parshin, A.Yu. Igumenov, Yu.L. Mikhlin, O.P. Pchelyakov, V.S. Zhigalov, 2016, published in Zhurnal Tekhnicheskoi Fiziki, 2016, Vol. 86, No. 9, pp. 136–140.

PHYSICAL ELECTRONICS

Electron Spectroscopy of Iron Disilicide

A. S. Parshin[a, *], A. Yu. Igumenov[a], Yu. L. Mikhlin[b], O. P. Pchelyakov[a,c], and V. S. Zhigalov[a,d]

[a] *Rechetnev Siberian State Aerospace University, ul. Krasnoyarskii rabochii 31, Krasnoyarsk, 660014 Russia*

[b] *Institute of Chemistry and Chemical Technology, Siberian Branch, Russian Academy of Sciences, Akademgorodok 50/24, Krasnoyarsk, 660036 Russia*

[c] *Rzhanov Institute of Semiconductor Physics, Siberian Branch, Russian Academy of Sciences, pr. Akademika Lavrent'eva 13, Novosobirsk, 630090 Russia*

[d] *Kirensky Institute of Physics, Siberian Branch, Russian Academy of Sciences, Akademgorodor 50/38, Krasnoyarsk, 660036 Russia*

**e-mail: aparshin2010@mail.ru*

Received October 26, 2015

Abstract—We have reported on the results of a complex investigation of iron disilicide $FeSi_2$ using characteristic electron energy loss spectroscopy, inelastic electron scattering cross section spectroscopy, and X-ray photoelectron spectroscopy. It has been shown that the main peak in the spectra of inelastic electron scattering for $FeSi_2$ is a superposition of two unresolved peaks, viz., surface and bulk plasmons. An analysis of the fine structure of the spectra of inelastic electron scattering cross section by their decomposition into Lorentz-like Tougaard peaks has made it possible to quantitatively estimate the contributions of individual energy loss processes to the resulting spectrum and determine their origin and energy.

DOI: 10.1134/S1063784216090176

INTRODUCTION

Iron disilicide $FeSi_2$ is of considerable interest for fundamental and applied studies [1–4]. Iron disilicide is obtained by molecular-beam epitaxy [5], thermal evaporation [6–9], and solid-phase and reactive epitaxy [7, 10, 11]. The physicochemical properties of Fe/Si_2 are analyzed by widely used methods of electron spectroscopy, including Auger-electron spectroscopy (AES) [4, 7, 8, 10–13], X-ray photoelectron spectroscopy (XPS) [1, 2, 6, 9, 10, 14], and characteristic electron energy loss (EEL) spectroscopy [4, 5–8, 10–13, 15–17].

In EEL spectroscopy, the energy of a bulk plasmon is used to identify various phases of silicides. According to different sources, the bulk plasmon energy for $FeSi_2$ amounts to 20.4–21.3 eV [7, 11–13, 16, 17].

Apart from the EEL spectroscopy, the spectroscopy of inelastic electron scattering cross section ($K\lambda$-spectroscopy) has been most often used in recent years to analyze the inelastic interaction of electrons with the substance. The $K\lambda$-spectra were calculated from experimental EEL spectra using the Tougaard–Chorkendorff algorithm [18] and contain only single energy losses with the intensity determined in absolute units. The inelastic electron scattering cross section spectroscopy has been used to test various materials [15, 18–32]. The advantages of the $K\lambda$-spectra as compared to EEL spectra was noted in [26–28]. A complex analysis of the Fe/Si system using the methods of EELS spectroscopy and inelastic electron scattering cross section spectroscopy is carried out in [15, 29, 30].

In this study, we report on the results of complex analysis of iron disilicide by the methods of EELS, $K\lambda$-spectroscopy, and XPS. The decomposition of experimental $K\lambda$-spectra into Lorentz-like Tougaard functions has made it possible to separate the loss peaks of the bulk and surface nature [31, 32].

1. EXPERIMENTAL TECHNIQUE

The $FeSi_2$ sample was prepared by fusing the silicon and iron mixture in an atomic ratio of 2 : 1 in a vacuum no worse than 10^{-4} Pa. X-ray diffraction analysis confirmed the single phase composition of the obtained alloy. We cut an approximately 1-mm-thick washer from the alloy and performed spectroscopic analysis.

The photoelectron spectra and integrated spectra of energy loss of reflected electrons were measured on ultra-high vacuum photoelectron spectrometer SPECS (Germany). The spectrometer was equipped with a spherical energy analyzer PHOIBOS MCD9, an X-ray tube with a twin diode as a source of Mg K_α

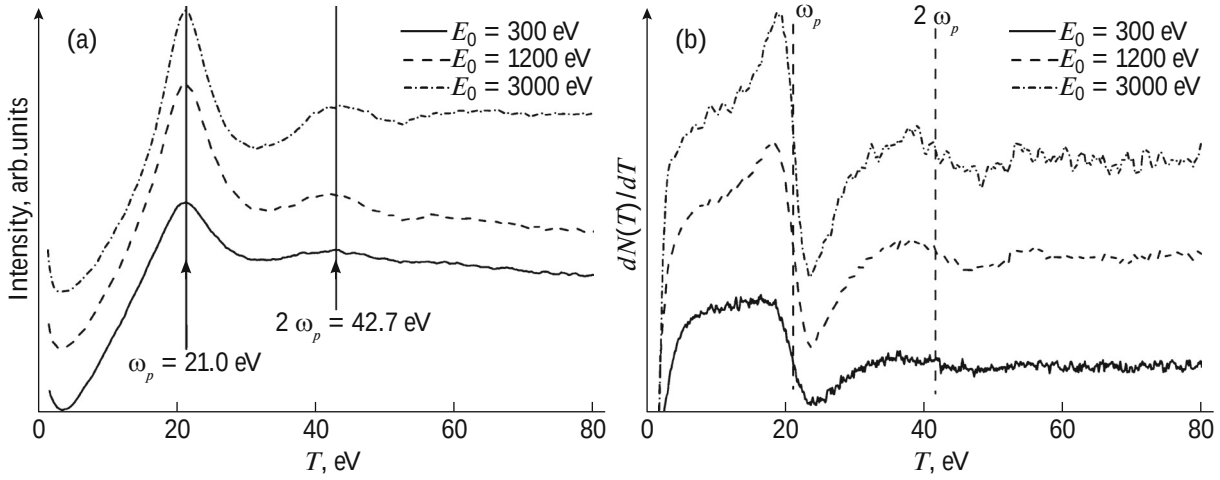

Fig. 1. (a) Integrated and (b) differential EEL spectra of $FeSi_2$ for different energies of primary electrons.

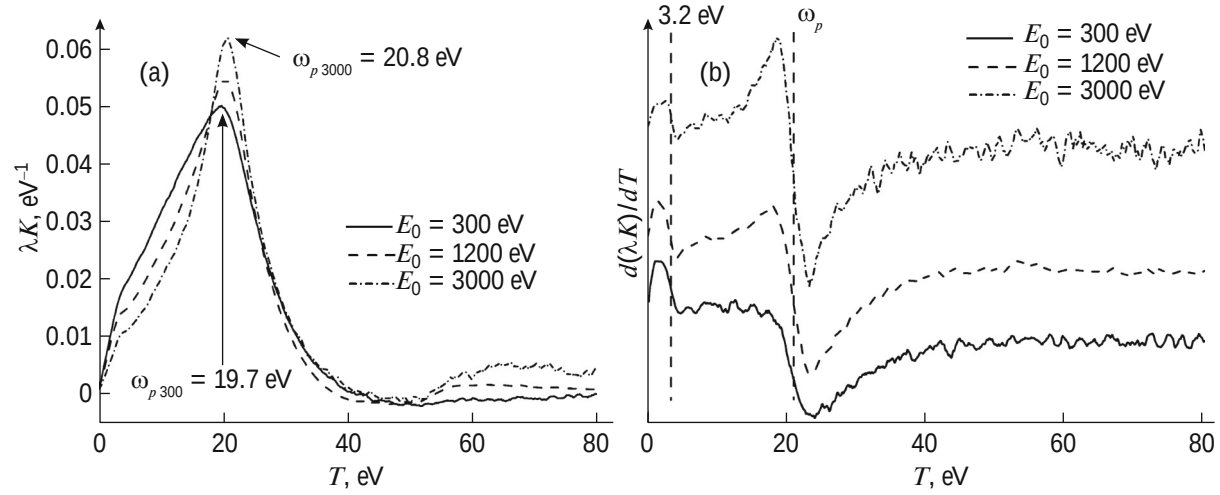

Fig. 2. (a) Integrated and (b) differential spectra of inelastic electron scattering cross section of $FeSi_2$.

X-ray radiation, and electron gun MicrofocusEK-12-M (STAIB Instruments) for exciting electron energy loss spectrum. Surface contamination was removed by etching with Ar^+ ions (accelerating voltage 2.5 kV, ion current 15 μA) using the PU-IQE-12/38 scanning ion gun (SPECS) directly in the spectrometer chamber prior to recording the electron spectra.

2. EXPERIMENTAL RESULTS

The X-ray photoelectron spectra of iron disilicide were obtained using Mg K_α radiation with an energy of 1253.6 eV. The atomic concentrations of Si and Fe atoms and carbon and oxygen impurity atoms were obtained from the survey spectra by the method of elemental sensitivity coefficients after subtracting of the background using the Shirley method. The total concentration of impurities after cleaning of the surface by ion etching did not exceed 15%. The ratio of atomic concentrations of silicon and ion was 0.66 : 0.34, which is close to the composition of the initial alloy mixture. We determined the binding energies of the 2*p* (Si) and 2*p* (Fe) photoelectron lines. Calibration was performed according to 1*s* carbon line with energy 285.0 eV. The binding energy of the 2*p* (Si) line was 99.7 eV. The binding energies of the $2p_{3/2}$Fe and $2p_{1/2}$ Fe doublet were 701.1 and 720.0 eV, respectively. The resultant values of the binding energy are in conformity with the available literature data for iron silicides [1, 2, 16].

The experimental spectra $N(T)$ of reflected electron energy losses in integrated form (Fig. 1a), where N is the number of reflected electrons that have lost energy T, were obtained in the range of 150 eV with a

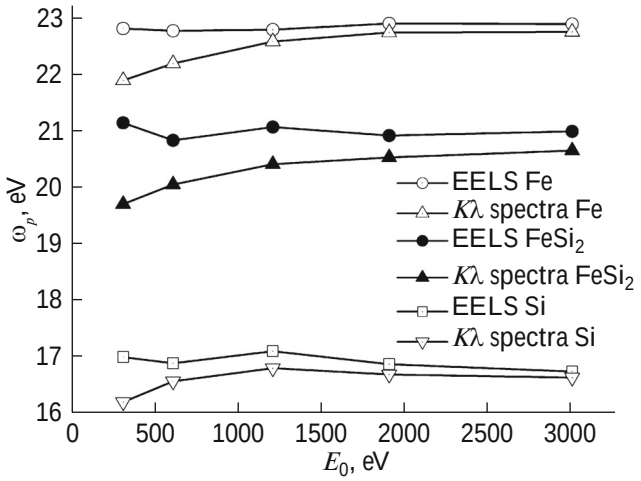

Fig. 3. Dependence of the bulk plasmon energies determined from the EEL spectra and spectra of the cross section of inelastic electron scattering on primary electron energies for Si, Fe, and $FeSi_2$.

step of 0.1 eV. Energy loss T was calculated as the difference between energy E_0 of primary electrons (zero losses) and energy E of reflected electrons, $T = E_0 - E$. The energies of primary electrons were 300, 600, 1200, 1900, and 3000 eV.

The integrated EEL spectra of $FeSi_2$ (see Fig. 1a) display two peaks, viz., an intense peak at energy 21 eV and a lower-intensity peak at 42.7 eV, corresponding to the excitation of single and double bulk plasmons in iron disilicide [7, 11–13, 16, 17]. The bulk nature of these peaks manifests in an increase in their relative intensity upon an increase in the energy of primary electrons. To determine the energies of the loss peaks more precisely and to reduce the effect of the structureless background, we performed a numerical differentiation of the $N(T)$ experimental curves (Fig. 1b).

The spectra of inelastic electron scattering (product of the average inelastic mean free path λ and differential inelastic scattering cross section $K(E_0, T)$) were obtained from the experimental energy loss spectrum for reflected electrons using the QUASESTM^{XS} REELS program package (quantum analysis of surface by electron spectroscopy cross sections determined by REELS) in accordance with the algorithm proposed in [18] (Fig. 2a). The spectra of the cross section of inelastic electron scattering reflect the probability of energy loss T by an electron upon single scattering over the inelastic mean free path per unit length. The heights of the peaks in these spectra determine the probabilities of single energy losses for surface or bulk excitations. The absolute values of the energy loss intensity in the spectra of inelastic electron scattering cross section make it possible to compare and analyze the spectra of different materials (including those obtained by different authors) without preliminary processing and normalization.

The main peak in the inelastic scattering cross section spectra for $FeSi_2$ (see Fig. 2a) is formed by two unresolved peaks (surface and bulk plasmons). This follows from the decreasing width of the spectrum at half amplitude from 19.1 to 12.5 eV upon an increase in the primary electron energy from 300 to 3000 eV. With increasing energy of primary electrons, the intensity of the bulk plasmon increases relative to the surface plasmon; as a result, the intensity of the low-energy region decreases.

The differential $K\lambda$-spectra for $FeSi_2$ are shown in Fig. 2b. Apart from the main peak in the $K\lambda$-spectra in the form of $d(\lambda K)/dT$, a singularity with energy 3.2 eV close to the energy of the interband transition is clearly observed in the EEL spectra of $FeSi_2$ [8, 17].

The energies of the peaks determined from the differential EEL spectra and the spectra of inelastic electron scattering cross section for $FeSi_2$ are shown in Fig. 3. The bulk plasmon energy is almost independent of the energy of primary electrons in the EEL spectra and increases monotonically with the energy of primary electrons in the spectra of inelastic electron scattering cross section spectra. Upon an increase in the energy of primary electrons, the depth of the yield of reflected electrons increases, which causes an increase in the intensity of bulk-like excitations and a decrease in the intensity of surface-like excitations, which in turn leads to a change in the shape and position of the peak in the spectra of inelastic electron scattering cross section.

A comparison of the EEL spectra with the spectra of the cross section of inelastic electron scattering shows that the shape of the $K\lambda$-spectra is more sensitive to an increase in the primary electron energy. This result can be associated with the subtraction of the background of multiple processes of inelastic scattering in the calculation of the $K\lambda$-spectra, which leads to an increase in the intensity of the surface-like excitations and their effect on the energy corresponding to the peak in the $K\lambda$-spectrum. Figure 3 also shows the energy of the bulk plasmon in the EELS and $K\lambda$-spectra on the energy of primary electrons for Si and Fe.

Thus, in determining the energies that correspond to the peaks in the $K\lambda$-spectra, the intensity of surface excitations can affect the resultant values.

3.1 Approximation of the Spectra of the Cross Section of Inelastic Electron Scattering Using Universal Tougaard Functions

To quantitatively estimate the contributions of different origins to the spectra of inelastic electron scattering cross section and to reliably determine their energies, we approximated the spectra for $FeSi_2$ by the three-parametric Lorentz-like Tougaard functions as follows [21, 31, 32]:

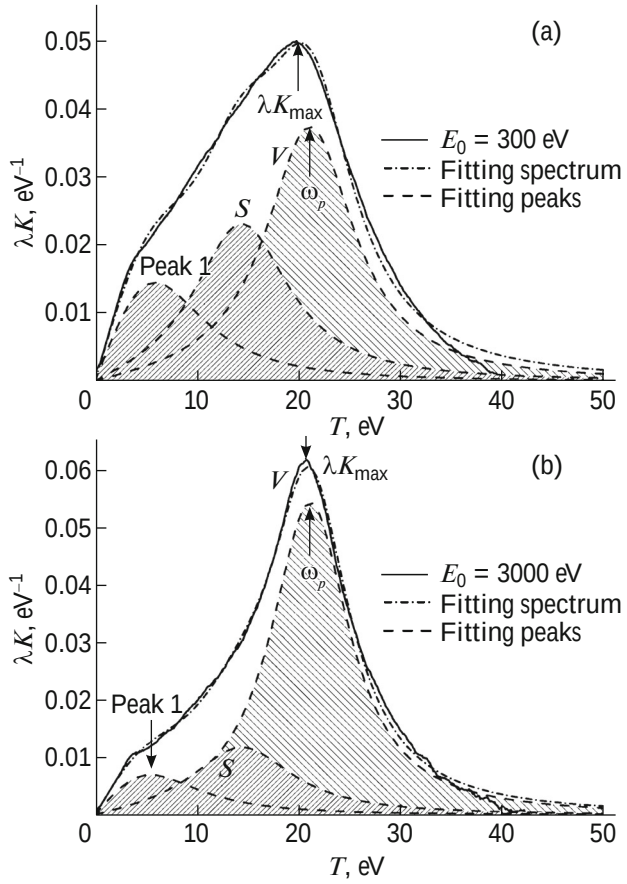

Fig. 4. Spectra of inelastic electron scattering cross section for $FeSi_2$ for primary electron energies of (a) 300 and (b) 3000 eV approximated by Lorentz-like Tougaard functions.

$$\lambda K = \frac{BT}{(C - T^2)^2 + DT^2}.$$

Parameter B determines the intensity of the peak, parameter C determines its position, and parameter D determines the width and indirectly affects the position and intensity of the peak. The description of the spectra of inelastic electron scattering cross section with the help of Lorentz-like functions (universal classes of the inelastic electron scattering cross section) was proposed by Tougaard [21].

An analysis of the processes of electron energy losses by separating contributions of different origins from the spectra of inelastic electron scattering cross section is a topical problem in electron spectroscopy, which can be used to estimate the effect of surface excitations on the EELS, XPS, and AES [23–28].

Figure 4 shows the results of an approximation of the spectra of inelastic electron scattering cross section for $FeSi_2$ for primary electron energies of 300 and 3000 eV. Since an analysis of the $K\lambda$-spectra of $FeSi_2$ revealed three types of contributions (bulk, surface, and weak low-energy contributions), we used three peaks for approximation (peaks *1*, *S*, and *V* in Fig. 4). The parameters of the Tougaard peaks were chosen in order to achieve the minimal standard deviation between the fitting and experimental spectra. The mean energies of the fitting peaks were 5.5, 14.4, and 21.1 eV. The ratio of the energies of the bulk and surface plasmons was 1.47, which is close to $\sqrt{2}$ in correspondence with the free electron gas approximation [34]. Low-energy peak *1* is close in energy to the interband transition in the EEL spectra of $FeSi_2$ [8, 17].

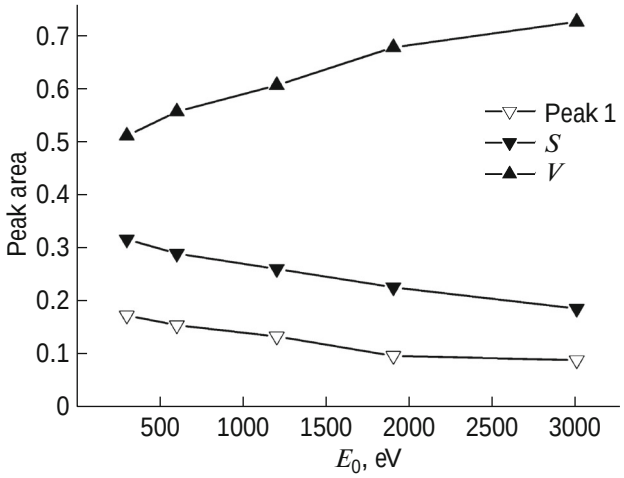

Fig. 5. Dependences of areas of fitting spectra on primary electron energy.

Figure 5 shows the dependence of the areas of the fitting peaks determining the intensity of excitations in the primary electron energy. Monotonically decreasing dependences of the areas of peaks *S* and *1* reflect their surface origin, while the opposite dependence of the area of peak *V* indicates its bulk origin.

The method of the decomposition of the spectra of the cross section of inelastic electron scattering into the peaks of losses makes it possible to quantitatively estimate the contributions of individual loss processes to the resultant $K\lambda$-spectrum and more precisely determine the loss energies of the characteristic peaks, which excludes the effect of the summation of intensities of unresolved peaks on the position of the resultant maximum.

CONCLUSIONS

We have analyzed the spectra of characteristic electron energy losses and of inelastic electron scattering cross section for $FeSi_2$. We have determined the energies that correspond to the loss peaks in the EEL spectra and in the spectra of inelastic electron scattering cross section; the energy of the peak in the EEL spectra is almost independent of the energy of primary electrons, while the energy that corresponds to the peak in the $K\lambda$-spectra increases with the primary

electron energy, which can be associated with the subtraction of the background of multiple energy losses in the calculation of the $K\lambda$-spectra. An analysis of the mechanisms of electron scattering and the quantitative estimation of the contribution of individual scattering processes to the $K\lambda$-spectra of $FeSi_2$ were carried out by analyzing the fine structure of the spectra of inelastic electron scattering cross section. The peaks of the surface and bulk origins were identified from the dependences of the areas of the fitting peaks on the primary electron energy.

REFERENCES

1. N. Ohtsu, M. Oku, K. Satoh, and K. Wagatsuma, Appl. Surf. Sci. **264**, 219 (2013).
2. N. Ohtsu, M. Oku, A. Nomura, T. Sugawara, T. Shishido, and K. Wagatsuma, Appl. Surf. Sci. **254**, 3288 (2008).
3. N. G. Galkin, D. L. Goroshko, E. A. Chusovitin, K. N. Galkin, and S. A. Dotsenko, Phys. Status Solidi C **10**, 1670 (2013).
4. N. G. Galkin, V. O. Polyarnyi, and A. S. Gouralnik, Thin Solid Films **464/465**, 199 (2004).
5. Q. Zhang, M. Tanaka, M. Takeguchi, M. Han, and K. Furuya, Jpn. J. Appl. Phys. **42**, 4667 (2003).
6. M. V. Gomoyunova, I. I. Pronin, D. E. Malygin, S. M. Solov'ev, D. V. Vyalykh, and S. L. Molodtsov, Tech. Phys. **50**, 1212 (2005).
7. J. M. Gallego and R. Miranda, J. Appl. Phys. **69**, 1377 (1991).
8. J. M. Gallego, J. V. Garcia, J. Alvarez, and R. Miranda, Phys. Rev. B **63**, 13 339 (1992).
9. R. Ayache, A. Bouabellou, F. Eichhorn, and F. Kermiche, J. Nano Adv. Mater. **2** (2), 51 (2014).
10. H. Moritz, B. Rösen, S. Popovi, A. Rizzi, and H. Lüth, J. Vac. Sci. Technol. B **10**, 1704 (1992).
11. J. Alvarez, J. J. Hinarejos, E. G. Michel, J. M. Gallego, A. L. Vazquez de Parga, J. de la Figuera, C. Ocal, and R. Miranda, Appl. Phys. Lett. **59**, 99 (1991).
12. A. Rizzi, H. Moritz, and H. Lüth, J. Vac. Sci. Technol. A **9**, 912 (1991).
13. X. Wallart, J. P. Nys, and C. Tetelin, Phys. Rev. B **48**, 5714 (1994).
14. M. Nikolaeva, M. Sendova-Vassileva, D. Dimova-Malinovska, D. Karpuzov, J. C. Pivin, and G. Beshkov, Vacuum **69**, 221 (2003).
15. P. Prieto, S. Hofmann, E. Elizalde, and J. M. Sanz, Surf. Interface Anal. **36**, 1392 (2004).
16. B. Egert and G. Panzner, Phys. Rev. B **29**, 2091 (1984).
17. V. G. Lifshits and Yu. V. Lunyakov, *EEL Spectra of Surface Phases on Silicon* (Dal'nauka, Vladivostok, 2004), p. 142.
18. S. Tougaard and I. Chorkendorff, Phys. Rev. B **35**, 6570 (1987).
19. S. Tougaard, Surf. Interface Anal. **11**, 453 (1988).
20. S. Tougaard and J. Kraaer, Phys. Rev. B **43**, 1651 (1991).
21. S. Tougaard, Surf. Interface Anal. **25**, 137 (1997).
22. G. Gergely, M. Menyhard, S. Gurban, A. Sulyok, J. Toth, D. Varga, and S. Tougaard, Solid State Ionics **47**, 141 (2001).
23. G. Gergely, Prog. Surf. Sci. **71**, 31 (2002).
24. G. Gergely, M. Menyhard, S. Gurban, A. Sulyok, J. Toth, D. Varga, and S. Tougaard, Surf. Interface Anal. **33**, 410 (2002).
25. G. T. Orosz, G. Gergely, S. Gurban, M. Menyhard, J. Toth, D. Varga, and S. Tougaard, Vacuum **71**, 147 (2003).
26. H. Jin, H. Yoshikawa, H. Iwai, S. Tanuma, and S. Tougaard, J. Surf. Anal. **15**, 321 (2009).
27. H. Jin, H. Shinotsuka, H. Yoshikawa, H. Iwai, S. Tanuma, and S. Tougaard, J. Appl. Phys. **107**, 083709 (2010).
28. H. Jin, H. Shinotsuka, H. Yoshikawa, H. Iwai, M. Arai, S. Tanuma, and S. Tougaard, Surf. Interface Anal. **45**, 985 (2013).
29. A. S. Parshin, G. A. Aleksandrova, A. E. Dolbak, O. P. Pchelyakov, B. Z. Ol'shanetskii, S. G. Ovchinnikov, and S. A. Kushchenkov, Tech. Phys. Lett. **34**, 381 (2008).
30. A. S. Parshin, S. A. Kushchenkov, G. A. Aleksandrova, and S. G. Ovchinnikov, Tech. Phys. **56**, 656 (2011).
31. A. S. Parshin, A. Yu. Igumenov, Yu. L. Mikhlin, O. P. Pchelyakov, A. I. Nikiforov, and V. A. Timofeev, Semiconductors **49**, 423 (2015).
32. A. Yu. Igumenov, A. S. Parshin, Yu. L. Mikhlin, O. P. Pchelyakov, A. I. Nikiforov, and V. A. Timofeev, Vestn. Sib. Gos. Aerokosm. Univ. **4** (56), 230 (2014).
33. http:// www.quases.com
34. H. Raether, *Surface Plasmons on Smooth and Rough Surfaces and on Gratings* (Springer, Berlin, 1988).

Translated by N. Wadhwa